

Accretion discs, MRI & the development of coherent structures

Evy Kersalé

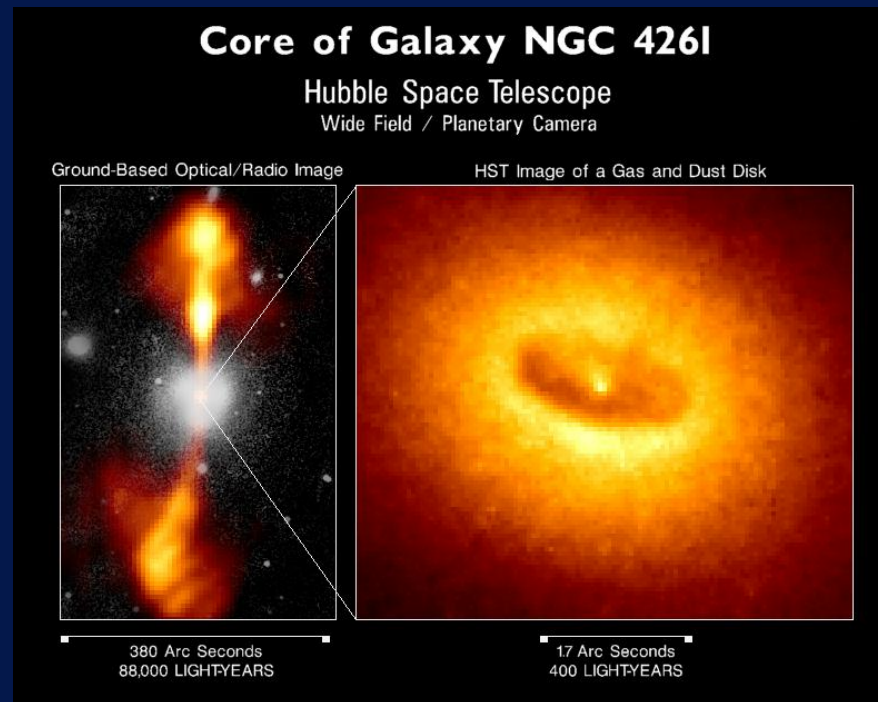
PPARC Postdoctoral Research Associate
Dept. of Appl. Math. — University of Leeds

Collaboration:

D. Hughes & S. Tobias (Dept. of Appl. Math., Leeds)
N. Weiss & G. Ogilvie (DAMTP, Cambridge)

Accretion in AGNs

Accretion consists in an accumulation of matter onto a massive central body



In Active Galactic Nuclei, accretion is the only mechanism able to release enough energy to produce large observed luminosity: $L \gtrsim 10^{47} \text{ erg s}^{-1}$ ($L_{\odot} = 10^{33} \text{ erg s}^{-1}$)

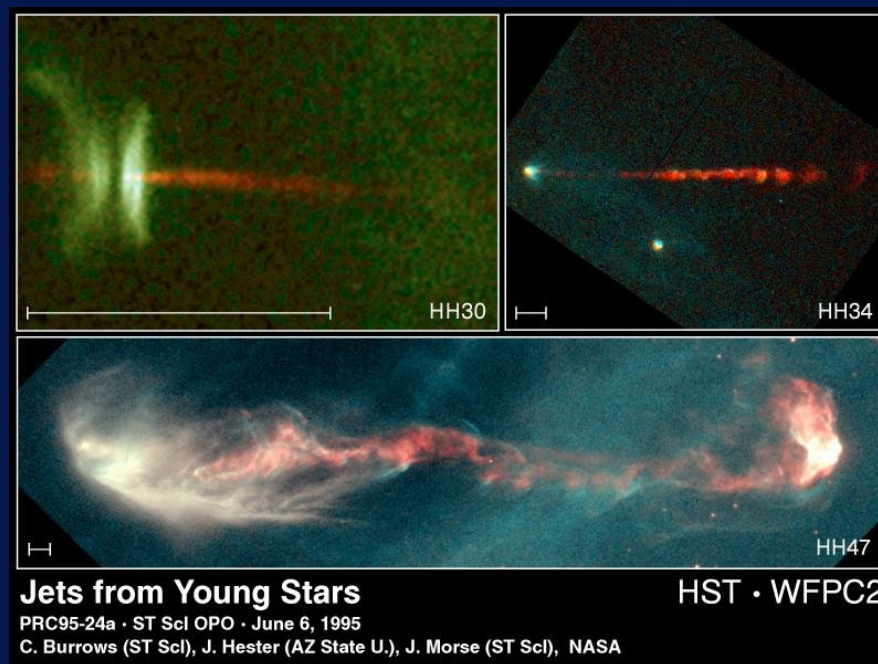
Energy released increases with compactness of the central body

$$\Delta\mathcal{E} = GM_{\star}m/R_{\star} \text{ with } M_{\star} \simeq 10^8 - 10^{10} M_{\odot}$$

Collimated ejection of matter often observed in relation with accretion processes

Young stars and planetary formation

Gravitational instabilities in interstellar molecular clouds lead to collapse of material and to the formation of a central dense bodies



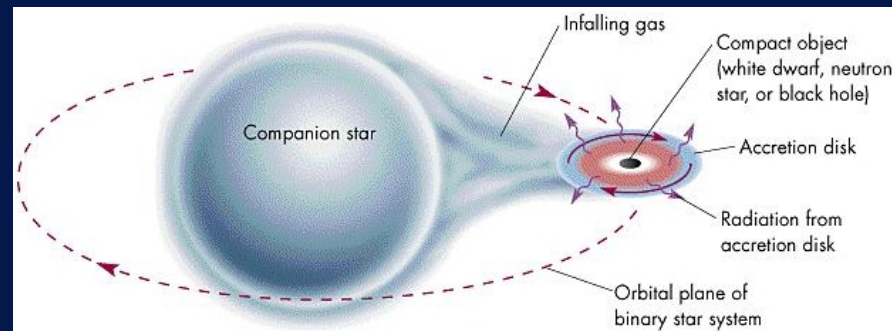
Matter accreted onto young stars form accretion discs (angular momentum conservation and radiative loss) that will eventually be sites of planetary formation

Collimated ejection of matter observed in relation with star formation

Magnetic fields observed in inner region of a protostellar accretion disc, $B \lesssim 1\text{kG}$ with strong toroidal component (Donati et al. 2005)

Accretion discs

Paradigm of accretion was first applied to studies of interacting binary stars (neutron star or black hole)



Angular momentum conservation leads to balance between gravity and centrifugal forces and hence to the formation of a disc

Orbiting gas can be accreted if angular momentum is removed by a torque acting on the disc (large scale jets) or within the disc

Shear viscosity fails in transporting angular momentum \Rightarrow effective shear due to interacting eddies in a turbulent flow needed

Which instability can drive turbulence in accretion discs?

Instabilities and turbulent transport in accretion discs

Turbulent transport of angular momentum arises from tight r - φ correlations in \mathbf{U} and \mathbf{B} :

- Tap into free energy source of differential rotation (i.e. sustain turbulence)

$$\frac{\partial \mathcal{E}_u}{\partial t} + \nabla \cdot \mathcal{F}_{\mathcal{E}_u} = -T_{r\varphi} \frac{d\Omega}{dr} \quad \text{where} \quad T_{r\varphi} = \langle \rho u_r u_\varphi \rangle - \langle B_r B_\varphi \rangle / \mu_0$$

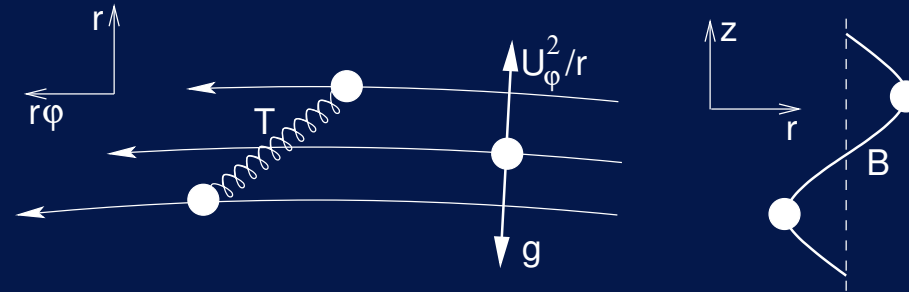
- Reynolds stress tensor $\propto \langle \rho u_r u_\varphi \rangle$ and Maxwell stress tensor $\propto -\langle B_r B_\varphi \rangle$ transport angular momentum

Onset of turbulence and transport enhancement:

- Hydrodynamic shear instabilities: Keplerian discs linearly stable [Rayleigh criterion, $d(r^2\Omega)/dr > 0$] but **finite amplitude instabilities still a matter of some controversy**
- Convection instabilities transport angular momentum inwards
- Papaloizou-Pringle instability (thick discs only): saturation in a strong spiral pressure wave (not in turbulence)
- Accretion-ejection instability, magnetic buoyancy, baroclinic & stratification effects
- **Magnetorotational instabilities lead to anisotropic turbulence, outwards transport of angular momentum and magnetic field amplification** (Velikhov 1959, Chandrasekhar 1960, Balbus & Hawley 1991)

Magnetorotational instabilities

Weakly magnetised ($\beta \gg 1$) rotating shearing flows unstable if $d\Omega/dr < 0$ (Balbus & Hawley 1998)



Local linear analysis (shearing sheet): Consider a local equilibrium around r_0 , $\mathbf{u}_0(x) = -q\Omega_0 x \mathbf{e}_y$, $\mathbf{B} = B_0 \mathbf{e}_z$ where $\Omega \propto r^{-q}$ and infinitesimal perturbations $(u_x, u_y, 0)$, $(b_x, b_y, 0) \propto \exp i(\omega t - kz)$

$$(\omega/\Omega_0)^2 = 2 - q + \frac{k^2 B_0^2}{\Omega_0^2} - \sqrt{(2 - q)^2 + 4 \frac{k^2 B_0^2}{\Omega_0^2}}$$

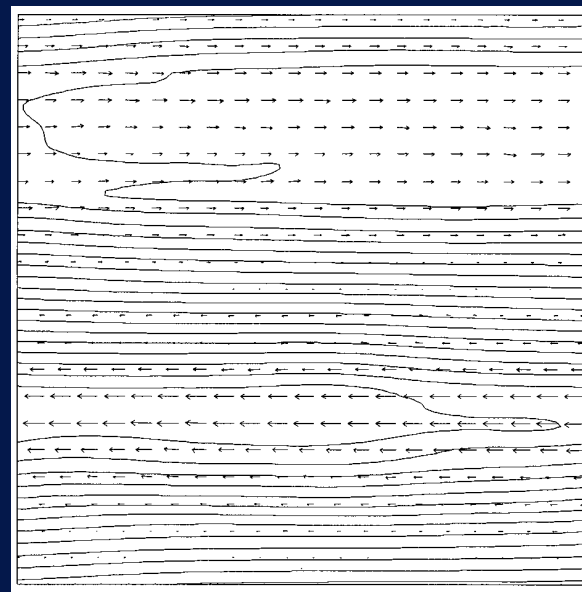
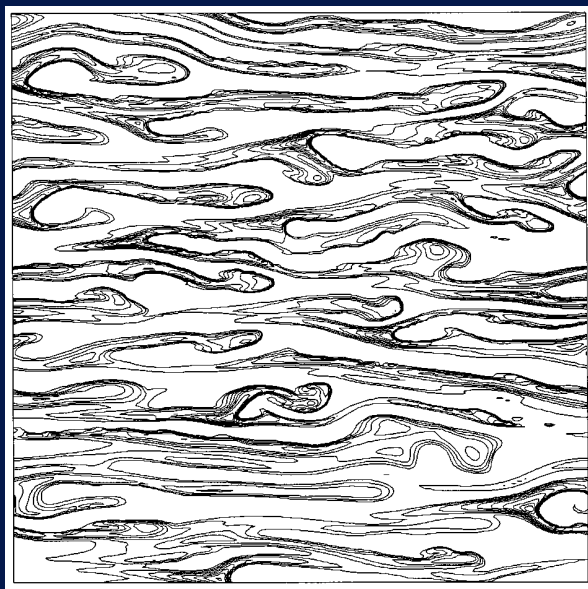
Instability ($\omega^2 < 0$) if $q > \frac{1}{2} \frac{k^2 B_0^2}{\Omega_0^2} > 0$ i.e. if the angular velocity decreases radially

$$\text{Maximal growth rate: } \frac{\gamma_{\max}}{\Omega_0} = \frac{q}{2} = -\frac{1}{2} \frac{d \ln \Omega}{d \ln r} \quad \text{for} \quad \frac{k^2 B_0^2}{\Omega_0^2} = q \left(1 - \frac{q}{4}\right)$$

In the absence of dissipative processes, instability occurs on a dynamical timescale for all $B_0 (\neq 0)$, however small, if $d\Omega/dr < 0$; γ_{\max} determined by the shearing flow only not by B_0

2-D axisymmetric computations: shearing box

Hawley & Balbus 1992

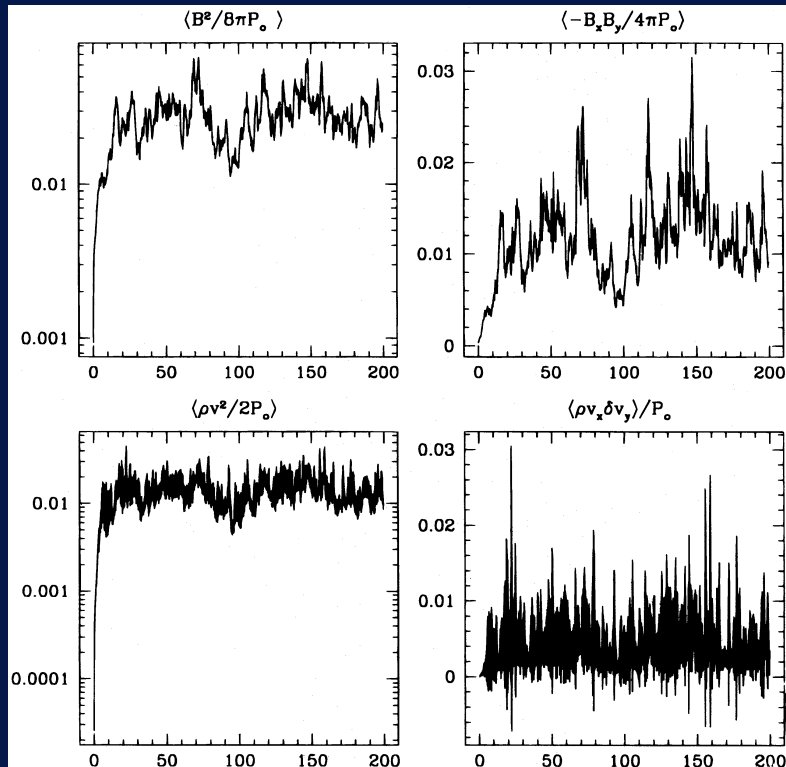


$\langle \mathbf{B} \rangle = 0$: Magnetic fields cannot be sustained because of the axisymmetry (no dynamo action); turbulence decaying on a resolution-dependent timescale

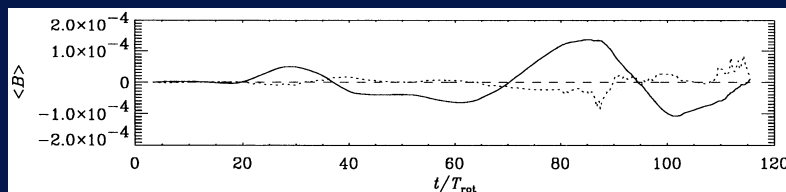
$\langle B_r \rangle \neq 0$: Fingering instability with small vertical length scale & large radial length scale

$\langle B_z \rangle \neq 0$: Preferred mode (“channel flow”), such that $\mathbf{u} \cdot \mathbf{B} = 0$, is also an exact non-linear solution (general property of incompressible fluids with perturbations proportional to a single Fourier mode) but it is unstable in 3-D (Goodman & Xu 1994)

Turbulence and dynamo action in 3-D



Hawley et al. 1996



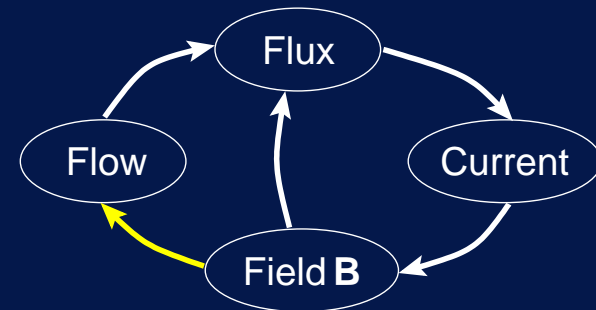
Brandenburg et al. 1995

Non-linear dynamics: ("periodic" boxes)

- Developed MHD turbulence with Reynolds & Maxwell stresses leading to outward transport of angular momentum
- Non-zero $\langle \mathbf{B} \rangle$ determines the saturation level of turbulence; even if B_φ always stronger (differential shear), $\langle B_z \rangle$ cannot be neglected
- No memory of initial B_z if $\langle B_z \rangle = 0$ but $\langle B^2 \rangle$ relies on the level of numerical dissipation

Dynamo action:

- MHD turbulence-driven (not HD shear turbulence)
- Bootstrapping process (mean-field theory does not apply)



- Large scale magnetic field

Numerical (and laboratory) experiments

Main numerical studies: local 2D & 3D, vertical stratification, full disc (torus)

Simulations of torus of accretion:

- Lack of resolution to solve small scale dynamics
- Run-down computations (no stationary state)

Shearing-box approximation:

- Local & periodic (semi-periodic radially)
- **Curvature neglected** but Coriolis & centrifugal forces included
- Angular velocity linearised: **vorticity gradient not taken into account**
- No net transport (radial symmetry)
- Periodicity implies strong constraints on the evolution of mean the magnetic field

Non-linear saturation mechanism & transport properties still to be elucidated

No systematic studies of mean field generation

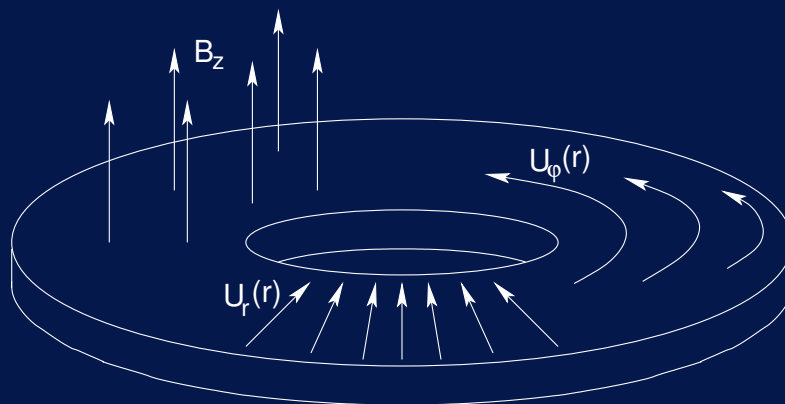
Laboratory experiments on liquid metal conducted in Princeton (PPPL), University of Maryland and Potsdam

Global model: annular section of an accretion disc

Modelling to address saturation mechanism of MRIs and nature of dynamo action

Key features of the model:

- Thin annular section (i.e. including curvature) as opposed to local shearing box
- Explicit treatment of dissipative processes (understanding of small scales dynamics)
- Permeable radial boundary conditions: permit accretion of matter and to reach a statistical stationary state



Magnetised Keplerian shearing flow driving accretion flow through viscous torque

Dimensionless evolution equations: incompressible ($\rho = 1$) non-ideal MHD

$$(\partial_t + \mathbf{U} \cdot \nabla) \mathbf{U} = -\nabla\Phi - \nabla\Pi + \mathbf{B} \cdot \nabla\mathbf{B} + \nu\nabla^2\mathbf{U}$$

$$(\partial_t + \mathbf{U} \cdot \nabla) \mathbf{B} = \mathbf{B} \cdot \nabla\mathbf{U} + \eta\nabla^2\mathbf{B}$$

$$\nabla \cdot \mathbf{B} = \nabla \cdot \mathbf{U} = 0$$

Length scaled with inner radius, r_i , time with Keplerian orbital period in r_i , $1/\sqrt{GM_*/r_i^3}$, and magnetic energy density with rotational kinetic energy density in r_i , $\rho GM_*/r_i$

Basic state: axisymmetric and z -invariant Keplerian ($\Omega \propto r^{-3/2}$) shearing flow **with accretion** threaded by a vertical magnetic field

$$U_r = -3\nu/2r, \quad U_\varphi = 1/\sqrt{r}, \quad U_z = 0, \quad B_r = B_\varphi = 0, \quad B_z = B_0, \quad \Pi = \delta - 9\nu^2/8r^2$$

Generalised pressure: no evolution equation for Π , so $\mathcal{P} = \Phi + \Pi$ may vanish and the disc may not be rotationally supported. `textcolorimport` Boundary conditions have either to enforce rotation or to bound pressure variations

Radial boundary conditions: **permeable** (no conditions on U_r and B_r)

$$\partial_r(\sqrt{r}U_\varphi) = 0, \quad \partial_r U_z = 0, \quad \Pi = \Pi_0, \quad \partial_r(rB_\varphi) = 0, \quad \partial_r B_z = 0$$

Linear stability theory

Numerical solution of linear evolution equations:

Linearisation: put $\{\mathbf{U}, \mathbf{B}, \Pi\} = \{\mathbf{U}_0, \mathbf{B}_0, \Pi_0\} + \varepsilon \mathcal{K}$, $\varepsilon \ll 1$ and neglect terms of order ε^2

Normal modes:

$$\mathcal{K}(\mathbf{r}, t) = \boldsymbol{\kappa}(r) \exp(\sigma t + im \varphi + ik z)$$

10th order differential linear system:

$$\sigma \mathcal{I}(r) \boldsymbol{\kappa}(r) = \mathcal{L}(r) \boldsymbol{\kappa}(r) \quad (\text{generalised eigenvalue problem})$$

Π evolves on much shorter time scales: $\nabla \cdot \mathbf{U} = 0 \Rightarrow \mathcal{I}_\pi = 0$

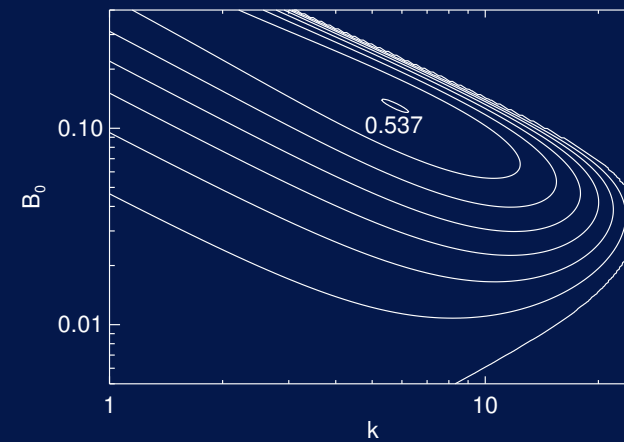
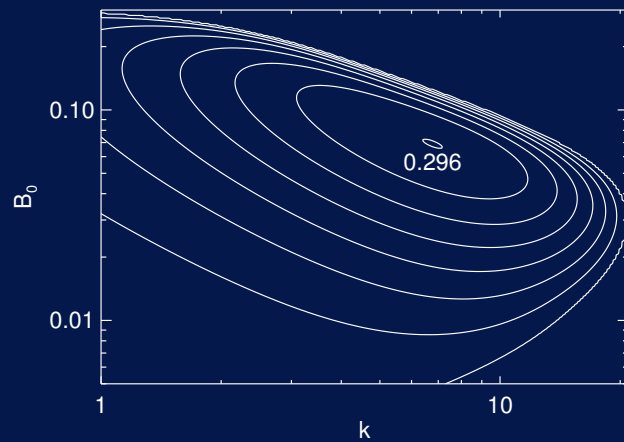
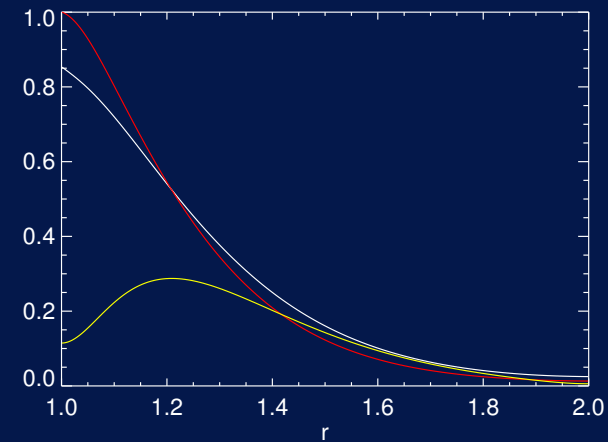
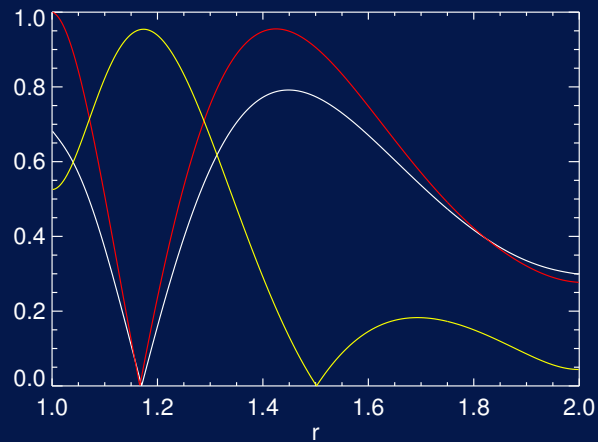
Linearised boundary conditions:

$$d_r(\sqrt{r}u_\varphi) = 0, \quad d_r u_z = 0, \quad \pi = 0, \quad d_r(r b_\varphi) = 0, \quad d_r b_z = 0$$

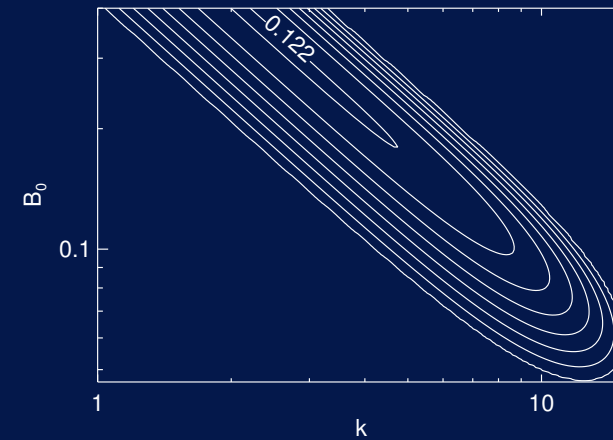
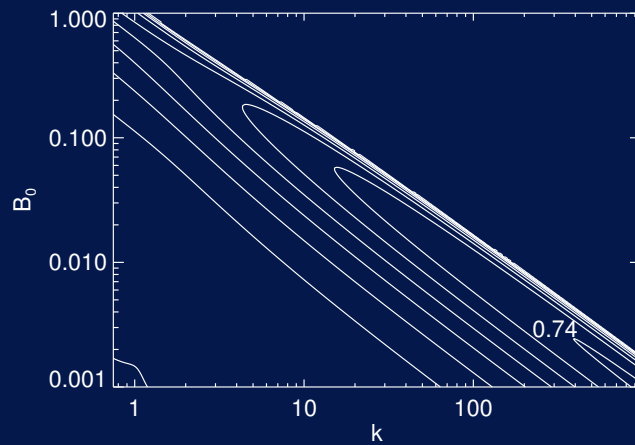
Numerical solution: inverse iteration and “shooting”

Unstable modes

Permeable radial boundaries permit the development of **wall-modes** as well as **body-modes**



Wall modes

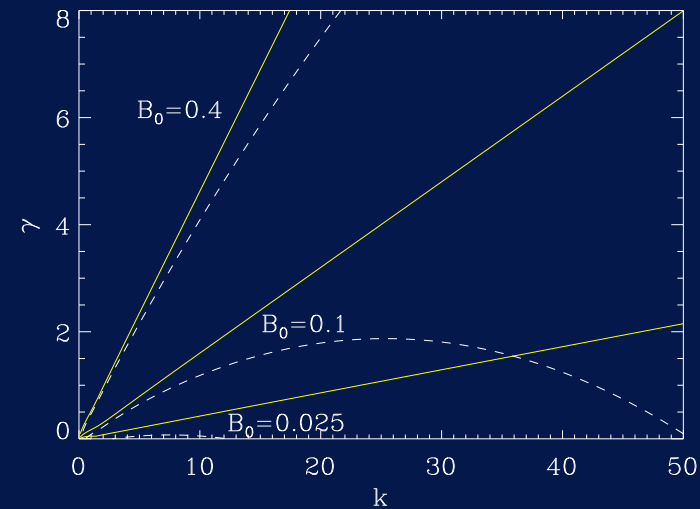
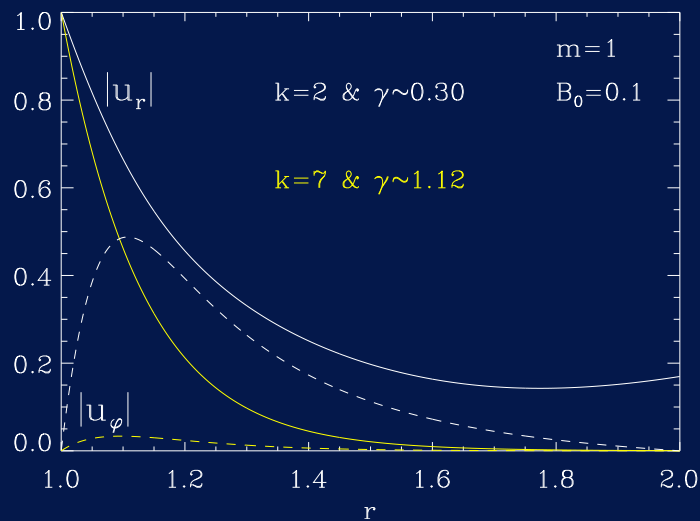


Properties of wall modes:

- Axisymmetric wall modes are the most unstable of all
- Local results recovered in the limit $k \rightarrow \infty$
- Large range of unstable azimuthal wave-numbers; range shrinks in the presence of strong B_φ
- Large parameter space survey (Kersalé et al. 2004)

Boundary conditions on U_φ instead of Π

Boundary condition $U_\varphi = U_{\varphi 0}$ (i.e. $u_\varphi = 0$) enhances instability of wall modes artificially



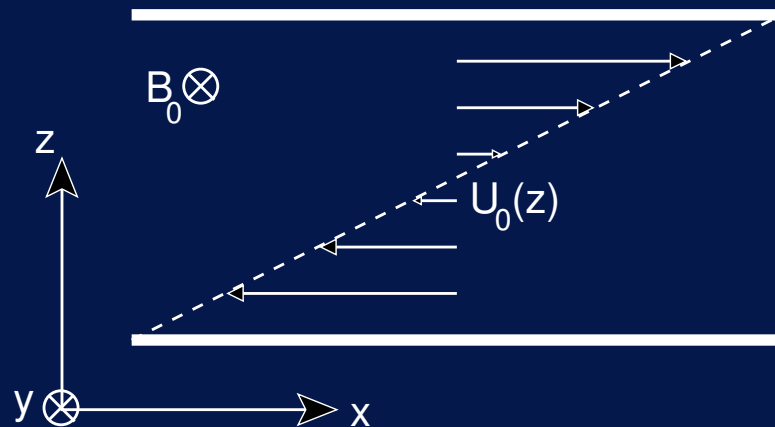
γ too large for the free energy available and large range of k : unstable

Ideal MHD: γ scales linearly with k and increases rapidly with B_0

Significant flux of energy through the boundaries to feed these modes

Inflow, curvature and Coriolis force not crucial

Cartesian linear shearing flow



Basic state:

$$\mathbf{U}_0 = z \mathbf{e}_x, \quad \mathbf{B}_0 = B_0 \mathbf{e}_y \quad \text{and} \quad \rho_0 = 1$$

2nd order system of linear ODEs: (incompressible, non dissipative MHD)

we consider normal modes $\underline{\mathcal{K}}(\mathbf{x}, t) = \underline{\kappa}(z) \exp(\sigma t + ik_x x + ik_y y)$

$$\chi \mathcal{H} u_x = -U_0' \mathcal{H} u_z - ik_x \pi$$

$$\chi \mathcal{H} u_y = -ik_y \pi$$

$$\chi \mathcal{H} u_z = -\pi'$$

$$0 = ik_x u_x + ik_y u_y + u_z'$$

where $\omega_a = kB_0$, $\chi = \sigma + ik_x U_0$ and $\mathcal{H} = \left(1 + \omega_a^2 / \chi^2\right)$

Cartesian wall modes: HD limit

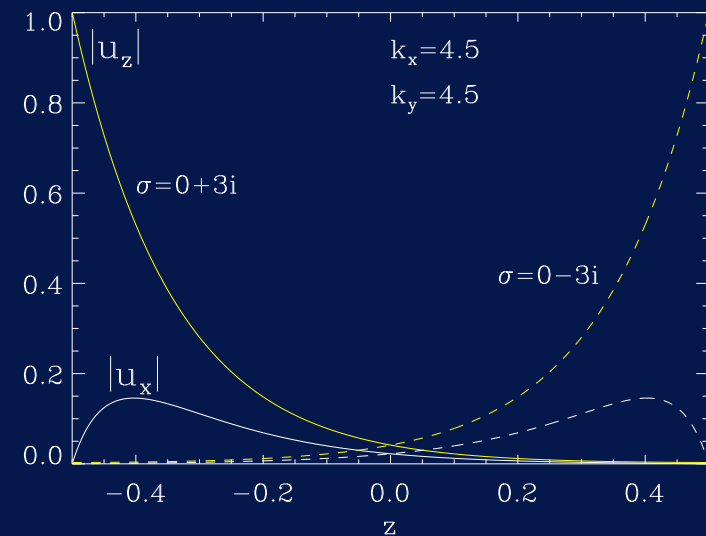
Hydrodynamic limit: $\omega_a = 0$ and $\mathcal{H} = 1$

HD modes are solutions of $\chi \left[u_z'' - \left(k^2 + \frac{\chi''}{\chi} \right) u_z \right] = 0$

Linear shear $\Rightarrow \chi'' = 0$ and $u_z = c_- \exp(-kz) + c_+ \exp(kz)$

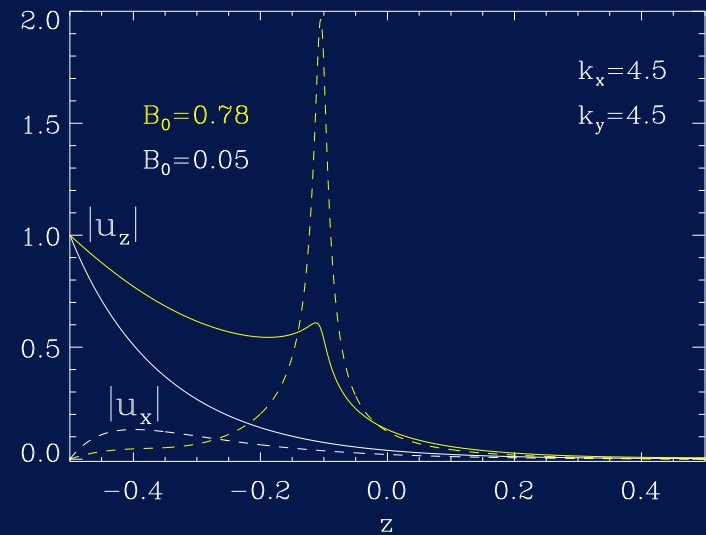
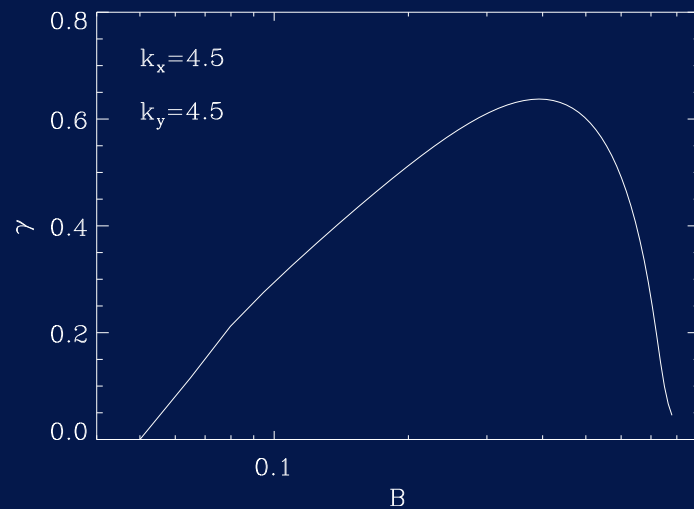
No discrete mode with the BCs $u_z = 0$, only a continuum of stable modes

Neutral wall modes solutions with BCs $u_x = 0$



Cartesian wall modes in MHD

Magnetic field destabilizes the wall modes



$$u_z'' - 2 \frac{\omega_a^2}{\chi^2 + \omega_a^2} \frac{\chi'}{\chi} u_z' - \left[k^2 + \frac{\chi''}{\chi} - 2 \frac{\omega_a^2}{\chi^2 + \omega_a^2} \left(\frac{\chi'}{\chi} \right)^2 \right] u_z = 0$$

Singularity when $\gamma = 0$ and $\omega = -k_x U_0 \pm \omega_a$

Non-linear evolution

Linear theory of prime importance in elucidating: • instability mechanism
• pertinent regimes of parameter

but complete understanding of MRIs attained only by investigating non-linear evolution

Only a few analytical non-linear results:

E.g. *Goodman & Xu 1994*: 2-D linear modes also solutions of the non-linear equations and 3-D stability of “channel flow” solutions

E.g. *Knobloch & Julien 2005*: fully non-linear equilibrated solution using asymptotic expansions

Although important, cannot capture all the complexity of non-linear evolution of MRIs

Imperative to make use of numerical computations

Numerical scheme: Space

- Requirements:
- explicit treatment of dissipative effects
 - cylindrical geometry
 - permeable boundary conditions

Pseudo-spectral method: **accurate & fast**

- Spectral decomposition: $X(r, \varphi, z) = \sum_{l,m,k} \mathcal{X}_{lmk} T_l(s) e^{im\varphi} \{\cos, \sin\}(kz)$,
with $T_l(s) = \cos(l \cos^{-1} s)$ & $2r = [(r_i - r_o) s + r_i + r_o]$, $s \in [-1, +1]$
- Differentiations performed using properties of trial functions
(Fourier: multiplication & Chebyshev: recurrence relations)
- Non-linear terms computed in configuration space making use of FFTs

Boundary conditions:

- Radial: Chebyshev-Tau (linear relations between the expansion coefficients)
- Azimuthal and vertical: Fourier-Galerkin (satisfied by trial functions)

Numerical scheme: Time

Advance in time: accuracy & stability

- Linear terms: Crank-Nicholson (implicit)
- Non-linear terms: 4th order Adams-Bashforth with adaptive time step (explicit)

$$\nabla^2 \Gamma^{n+1} = \nabla \cdot \mathcal{N}_u^n$$

$$[\mathcal{I} - \Theta \delta t \mathcal{L}] \mathbf{U}^{n+1} = -\nabla \Gamma^{n+1} + \mathcal{N}_u^n + [\mathcal{I} + (1 - \Theta) \delta t \mathcal{L}] \mathbf{U}^n$$

$$[\mathcal{I} - \Theta \delta t \mathcal{L}] \tilde{\mathbf{B}}^{n+1} = \mathcal{N}_b^n + [\mathcal{I} + (1 - \Theta) \delta t \mathcal{L}] \mathbf{B}^n$$

$$\mathbf{B}^{n+1} = \tilde{\mathbf{B}}^{n+1} - \nabla \Psi \quad \text{with} \quad \nabla^2 \Psi = \nabla \cdot \tilde{\mathbf{B}}^{n+1}$$

With $\Theta \in [0, 1]$, $\Gamma = \delta t \Pi$, $\mathcal{L} = \nu \nabla^2$ and \mathcal{N} represents the nonlinear terms

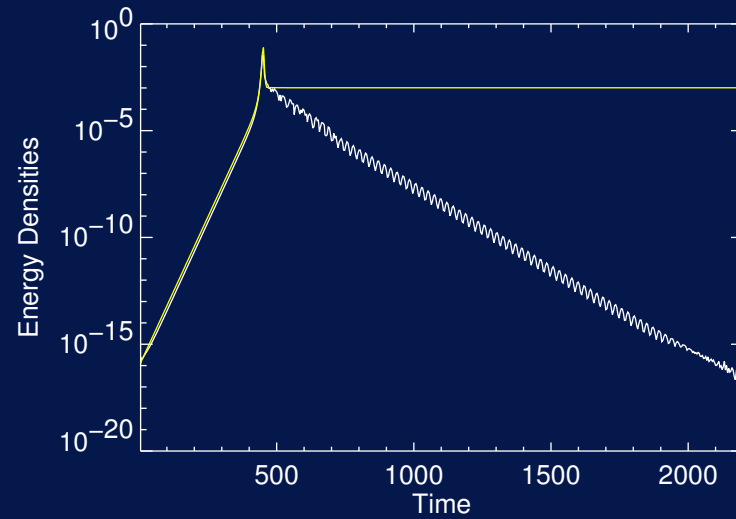
- Differential operator $(\mathcal{I} - \Theta \delta t \mathcal{L})$ non trivial (Chebyshev polynomials in an annulus)
- Divergence-free constraints give boundary conditions to compute U_r and B_r

Non-linear evolution of axisymmetric wall modes

Numerical investigation:

- Basic state: Keplerian shearing flow
viscosity-driven accretion
uniform vertical magnetic field
- Parameter space survey: $R_o = \{2, 4\}$, $H = 0.5$,
 $B_0 \simeq 10^{-1}$ - 10^{-2} , $\nu = \eta \simeq 3.5 \times 10^{-3}$ - 10^{-4}
- Parameter values chosen such that **only one wall mode linearly unstable**
- Instability triggered by random small amplitude perturbations of U_φ
- Exponential growth in agreement with linear theory
- **Non-linear behaviour mediated by coherent structures:**
 - suppression of MRIs
 - cyclic evolution
 - relaxation to a non trivial steady state

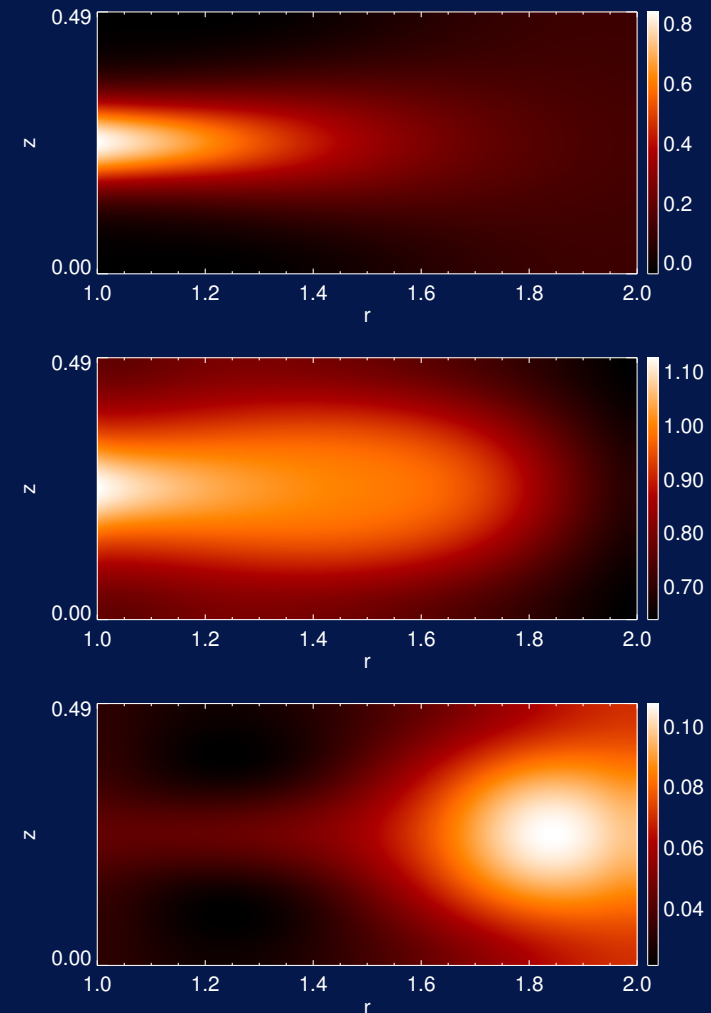
Self-consistent suppression of the instability



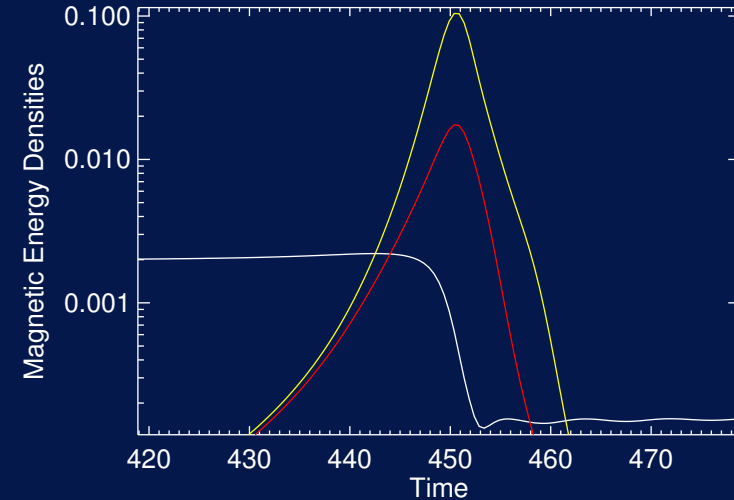
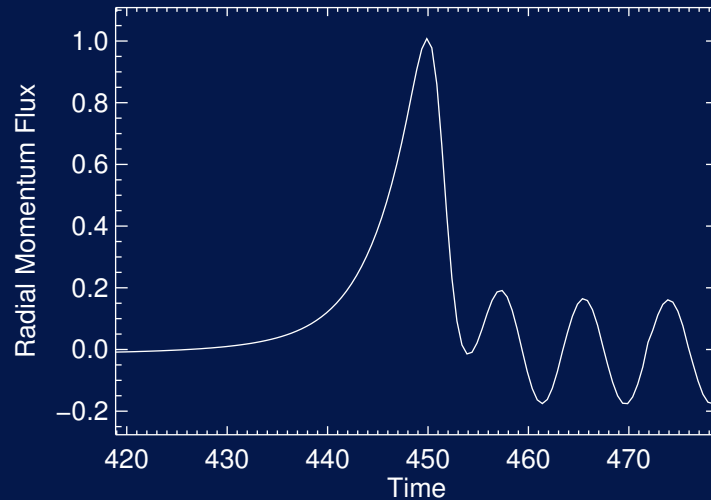
Evolution:

- Exponential growth
- Non-linear readjustments
- Relaxation to a different stable Keplerian equilibrium

Coherent radial jet transports magnetic flux outwards



Removing of magnetic flux



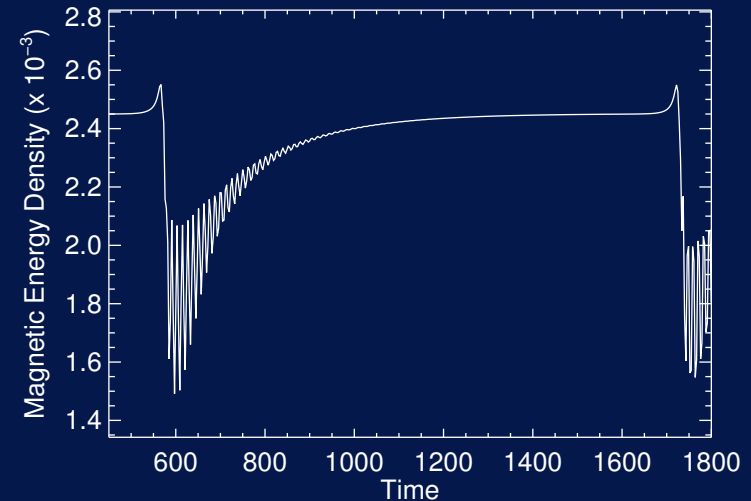
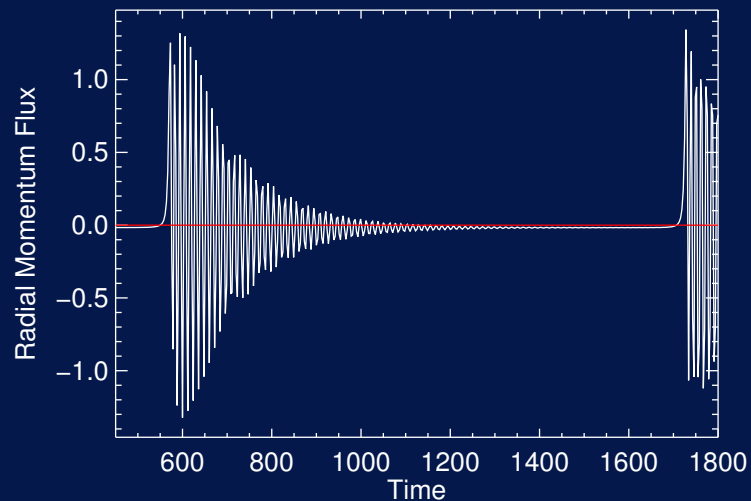
Non linear behaviour:

- Formation of a **fast** radial jet: outwards flux of momentum
- Super-exponential growth of the magnetic energy
- **Advection of vertical magnetic field** out of the domain
- Drop in vertical magnetic field leads to **instability suppression**
- Whole disc undergoes epicyclic oscillations (damped on a dissipative timescale)

Relaxation to a stable equilibrium: initial Keplerian flow (with accretion) with a reduced uniform magnetic field

Radial extension of the disc

Preventing magnetic removal of flux by increasing radial extent of the disc



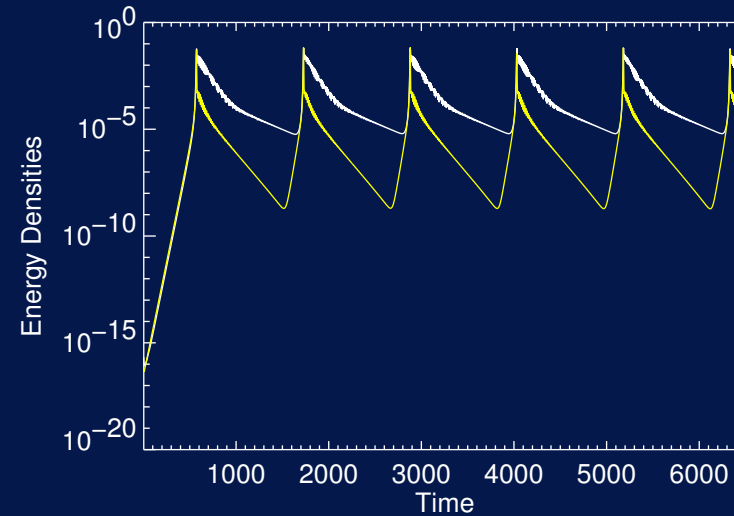
Strong radial jet: – Transports B_z -flux outwards; storage in stable part of the disc
 – Switches-off the instability
 – Produces large amplitude epicyclic oscillations (viscous damping)

Accretion: – Brings B_z -flux towards the centre
 – Relaxation to initial unstable state

Process leads to a net flux of radial momentum outwards

Relaxation oscillator

- Strong radial jet but no B_z -flux expelled:
- **Cyclic behaviour** (periodic)
 - **Multiple timescales**

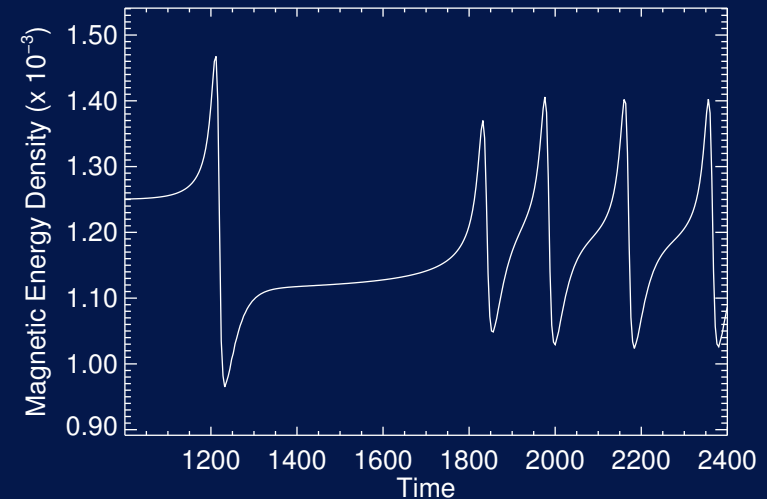
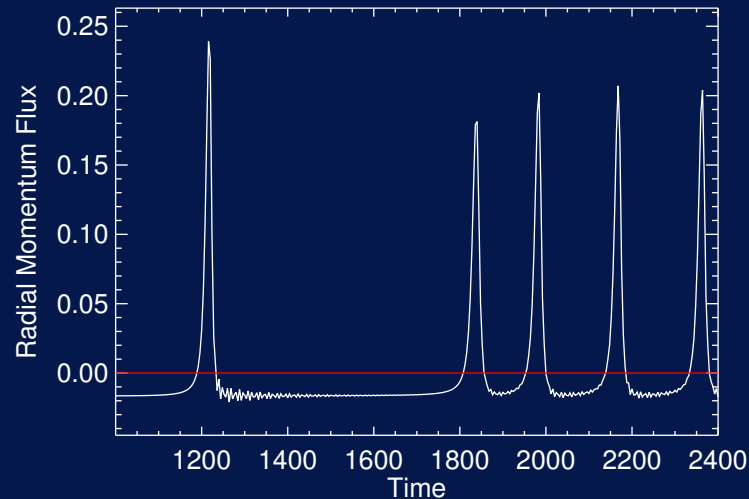


Dynamics successively linear and non-linear:

- Exponential growth (linear instability)
- Rapid non-linear readjustments on a dynamical timescale (strong radial jet)
- Dissipative relaxation to the initial unstable equilibrium on a viscous timescale

Reducing the strength of the jet

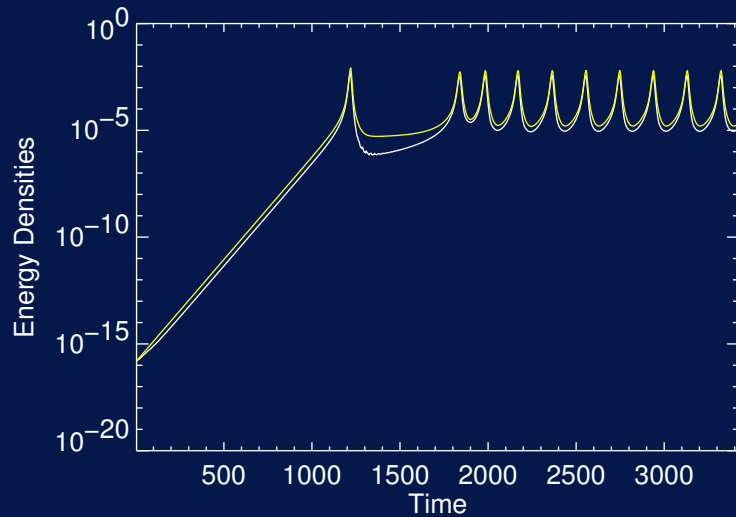
Preventing removal of magnetic flux by decreasing the strength of the non-linear jet



Successive phases — radial jet & accretion: **net flux of radial momentum outwards**

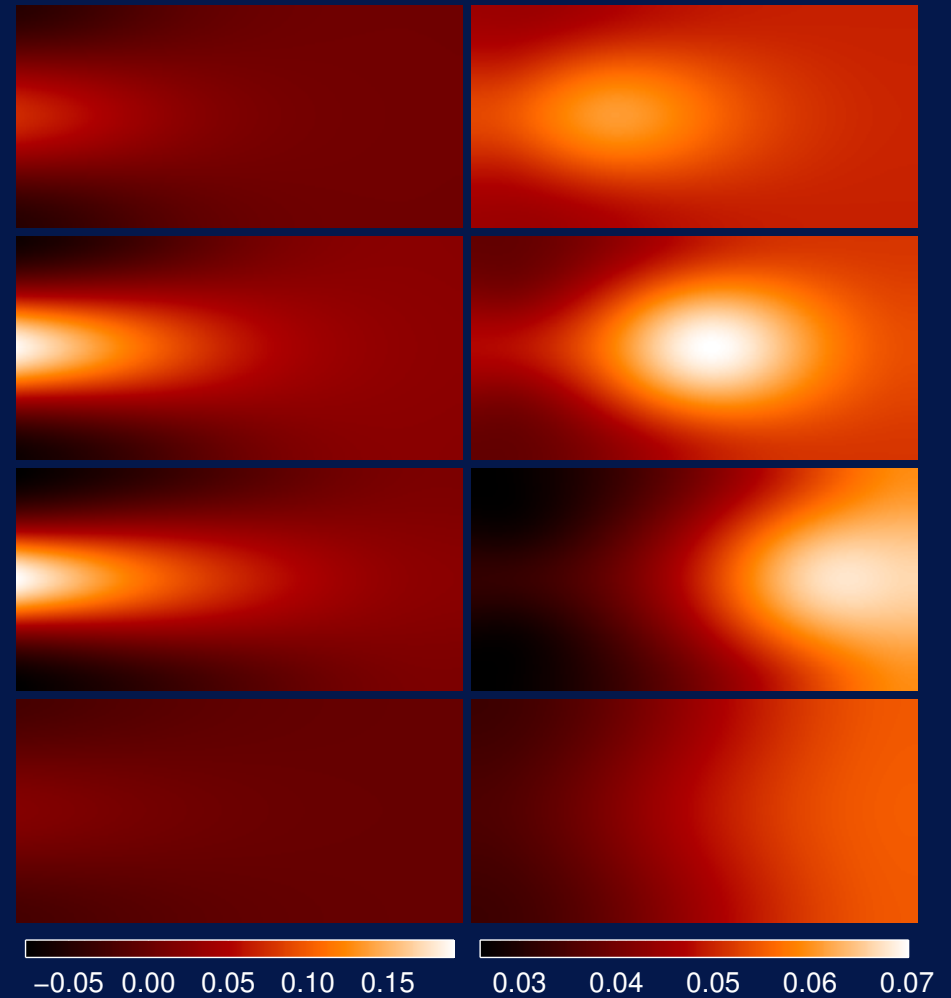
- **Smoother non-linear events** (no large amplitude epicyclic motions)
- Partial loss of B_z -flux but readjustment of the system (robust process)
- **Relaxation to a periodic solution**
- Oscillations around a new equilibrium (not the initial Keplerian state)

Fully non-linear oscillations



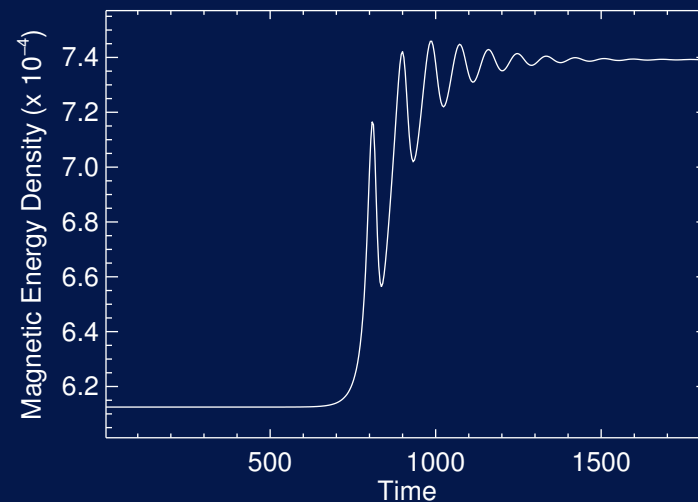
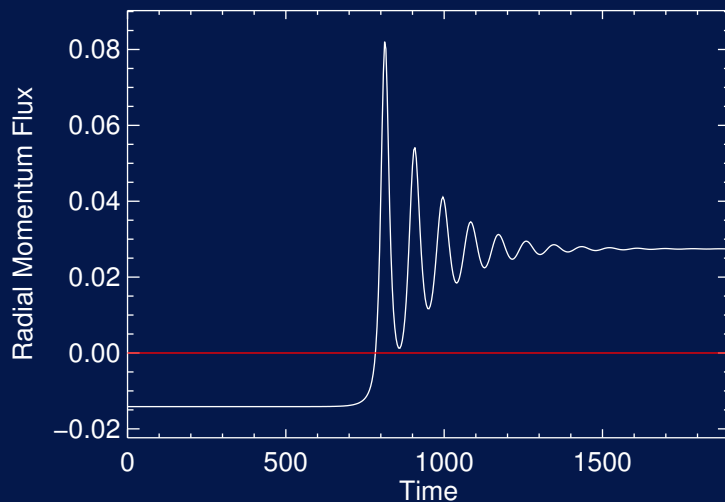
Fully non-linear dynamics:

- Interval between bursts shorter than a dissipative timescale
- No relaxation to Keplerian state
- Competition between non-linear jet and accretion



Further reduction of jet strength

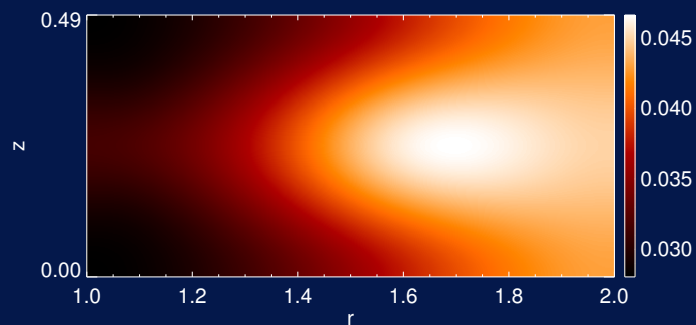
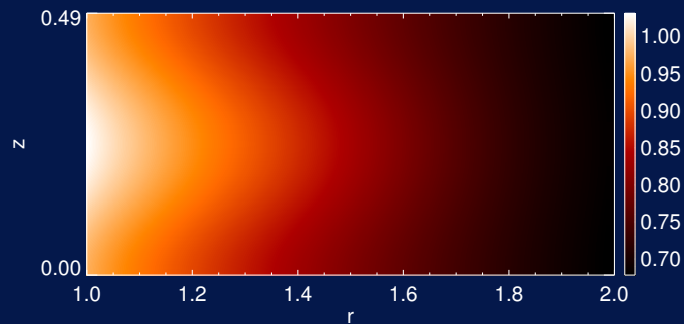
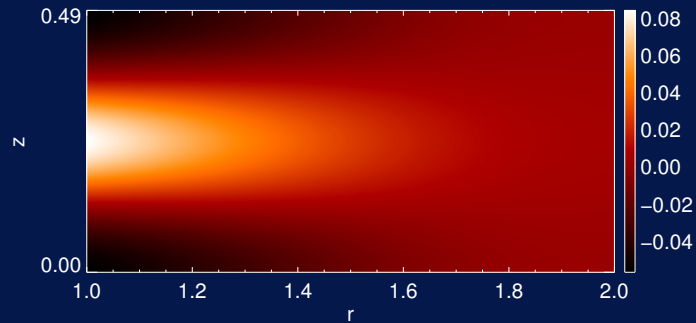
Timescale of non-linear processes sufficiently long to permit a smooth reorganisation of the system



Evolution of the unstable wall mode:

- Linear regime (MRI does not contribute to the transport)
- **Weak non-linear jet** evolving on a dynamical timescale
- Transient phase non-linear adjustments on a dissipative timescale
- **Relaxation to a non-trivial stable equilibrium:** Increased magnetic energy
Outwards flux of radial momentum

Non-trivial stable stationary state



Final state:

- Radial jet
- Non-Keplerian shearing flow
- Non-uniform magnetic field (B_r , B_φ , B_z)

MRI still in action: generate Reynolds and Maxwell stresses

Transport of angular momentum

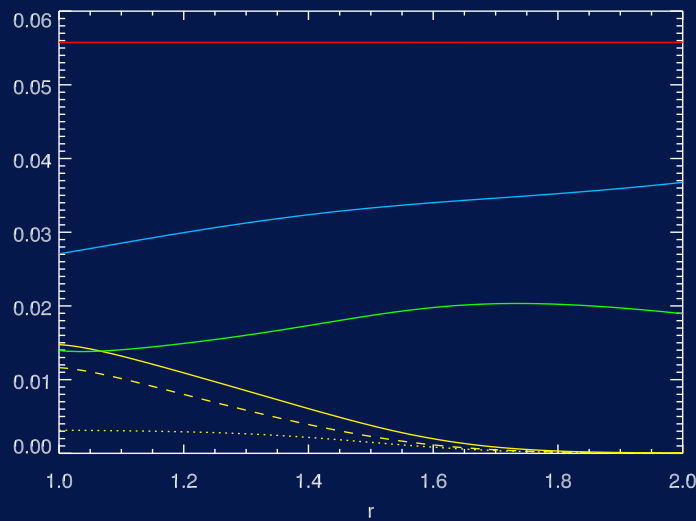
Split the velocity field into mean and fluctuating parts with respect to vertical averaging:

$$\mathbf{u}(r, z, t) = \bar{\mathbf{u}}(r, t) + \mathbf{u}'(r, z, t) \quad \text{with} \quad \int_0^H \mathbf{u}' dz = 0$$

Conservation of angular momentum in 1-D:

$$\frac{\partial \lambda \bar{l}}{\partial t} + \lambda \bar{u}_r \frac{\partial \bar{l}}{\partial r} = -\frac{\partial}{\partial r} \left[\frac{r \lambda}{H} \int_0^H \left(u'_r u'_\varphi - B_r B_\varphi - \nu \lambda r^2 \frac{\partial \Omega}{\partial r} \right) dz \right] \equiv -\frac{\partial \bar{G}}{\partial r}$$

with the linear density of mass $\lambda = 2\pi r \rho H$ and the specific angular momentum $l = r u_\varphi \simeq \sqrt{r}$



As expected, viscous, Reynolds and Maxwell stresses are positive

MRIs develop preferentially in the inner region and hence produce a positive torque

Stationary state: $\lambda \bar{u}_r = -\partial_r \bar{G} / \partial_r \bar{l}$, with $\partial_r \bar{l} < 0$

Stationary state for incompressible flows: $\partial_r (\lambda \bar{u}_r \bar{l} + \bar{G}) = 0$ since $\lambda \bar{u}_r$ is always constant

Conclusions & Prospects

Non-linear evolution of MRIs leading to:

- cyclic behaviours
- trivial or non-trivial equilibria

Saturation of the MRI relies on magnetic flux redistribution by non-linear coherent structures

Model requires **key features** to find the solutions calculated:

- cylindrical geometry (in & out)
- explicit treatment of dissipative processes
- permeable boundary conditions
- ability to reach a steady state (no run-down computation)

Correct computation of the evolution of MRIs on very **different timescales** (dynamical & dissipative)

Transition to less coherent — turbulent — regimes at higher Reynolds numbers:

- 2-D Kelvin-Helmholtz
- 3-D coherent structures unstable to non-axisymmetric perturbations

Stable 2-D structures identified are building blocks: **3-D chaotic flows may well exhibit some properties of 2-D stable solutions** (in a statistical sense)